



## Symmetry analysis of possible superconducting states in $K_xFe_ySe_2$ superconductors

I. I. Mazin\*

Code 6393, Naval Research Laboratory, Washington, D.C. 20375, USA

(Received 4 May 2011; revised manuscript received 8 June 2011; published 25 July 2011)

A newly discovered family of Fe-based superconductors is isostructural with the so-called 122 family of Fe pnictides but has a qualitatively different doping state. Early experiments indicate that superconductivity is nodeless, yet prerequisites for the  $s_{\pm}$  nodeless state (generally believed to be realized in Fe superconductors) are missing. It is tempting to assign a  $d$ -wave symmetry to the new materials, and it does seem, at first glance, that such a state may be nodeless. Yet a more careful analysis shows that it is not possible, given the particular 122 crystallography. If indeed superconductivity in this system is nodeless, the possible choice of admissible symmetries is severely limited: it is either a conventional single-sign  $s_+$  state or another  $s_{\pm}$  state, different from the one believed to be present in other Fe-based superconductors.

DOI: [10.1103/PhysRevB.84.024529](https://doi.org/10.1103/PhysRevB.84.024529)

PACS number(s): 74.20.Pq, 74.25.Jb, 74.70.Xa

Recent reports of superconductivity at  $T_c$  in excess of  $35\text{ K}^1$  in iron based superconductors (FeBS) isostructural with  $BaFe_2As_2$  (the so-called 122 structure), but with Se instead of As, have triggered a new surge of interest among the physics community. These materials are believed by many to open a new page in Fe-based superconductivity (see Ref. 2 for a brief review). Indeed, the stoichiometric composition,  $AFe_2Se_2$ , where A is an alkali metal, corresponds to a formal doping of 0.5 electron off the standard for FeBS parent compound ( $LaFeAsO$ ,  $BaFe_2As_2$ , or  $FeSe$ ) valence state of iron,  $Fe^{2+}$ . Such a large doping in other materials, such as  $Ba(Fe,Co)_2As_2$ , leads to complete suppression of superconductivity, which has been generally ascribed<sup>3,4</sup> to disappearance of the hole pockets of the Fermi surface and formal violation of the quasineesting condition for the  $s_{\pm}$  superconductivity.

Indeed all band structure calculations show<sup>5</sup> that in  $AFe_2Se_2$  the hole bands are well under the Fermi surface (for the reported experimental crystal structure of  $KFe_2Se_2$ , about 60 meV), and this is confirmed by preliminary ARPES results.<sup>6-8</sup> This has led to various speculations<sup>9-11</sup>, in particular that in this subfamily it is not the familiar  $s_{\pm}$  superconductivity that is realized, but a  $d$ -wave superconductivity<sup>6,9,10</sup> of the sort discussed in an early paper by Kuroki *et al.*<sup>12</sup> Unfortunately, these speculations are entirely based on the “unfolded” Brillouin zone (BZ) description of the electronic structure, a simplified model that neglects the symmetry lowering due to the As or Se atoms and the fact that in the real unit cell there are two Fe ions, not one. Furthermore, they implicitly assume that spin susceptibility corresponding to the “checkerboard” wave vector,  $Q = (\bar{\pi}, \bar{\pi})$ , is substantially enhanced, despite the fact that this vector corresponds to an electron-electron interband transition that is much less efficient in enhancing susceptibility than electron-hole transitions (here and below, we use an over bar when we work in the unfolded BZ). This assumption is supported by model calculations based on an on-site Hubbard Hamiltonian,<sup>9</sup> but applicability of this Hamiltonian to FeBS (including pnictides) is still an open question.

In this paper, we critically address these two assumptions and show that the latter assumption is supported by first principles calculations, but the former assumption is actually very misleading. We present a general symmetry analysis of possible superconducting symmetries supported by the Fermi

surface topology existing in  $AFe_2Se_2$ . This analysis is not limited by a specific density functional calculation but is based on the general crystallographic considerations appropriate for this crystal structure. It appears that it is impossible to fold down a nodeless  $d$ -wave state so as to avoid formation of line nodes. Thus, emerging experimental evidence from ARPES,<sup>6-8</sup> specific heat,<sup>13</sup> NMR,<sup>14</sup> and optics<sup>15</sup> that superconductivity in  $AFe_2Se_2$  is nodeless is a strong argument against a  $d$  wave. A conventional  $s$  state is also unlikely based on the proximity to magnetism and actual observation of a coexistence of superconductivity and magnetism. We emphasize that the symmetry of the folded Fermi surfaces does allow for a nodeless state, which, however, has an overall  $s$  symmetry and can also be called  $s_{\pm}$ , as it is strongly sign changing. Unlike the  $s_{\pm}$  advocated for the “old” FeBS, it is not driven by  $(\bar{\pi}, 0)$  spin fluctuations and cannot be derived from considering an unfolded BZ Fermi surface.

The unfolded Fermi surface topology in materials with the 122 structure is controlled by two factors: ellipticity of individual electron pockets and their  $k_z$  dispersion (Fig. 1). The ellipticity in the unfolded zone is determined by the relative position of the  $xy$  and  $xz/yz$  levels of Fe and the relative dispersion of the bands derived from them. Indeed,<sup>16</sup> the point on the Fermi surface located between  $\bar{\Gamma}$  and  $\bar{X}$  has a purely  $xy$  character, while that between  $\bar{\Gamma}$  and  $\bar{M}$  has a pure  $yz$  character. At the  $\bar{X}$  point the  $xy$  state is slightly below the  $yz$  state but has a stronger dispersion; therefore, depending on the system parameters and the Fermi level, the corresponding point of the Fermi surface may be more removed from  $\bar{X}$ , or less. In the 1111 compounds, the first to have been investigated, the dispersion of the  $xy$  band is not high enough to reverse the natural trend, so the Fermi surface remains elongated in the  $\bar{\Gamma}\bar{X}$  (1,0) direction.

For both  $xy$  and  $xz/yz$  bands the hopping mainly proceeds via As (Se)  $p$  orbitals. The  $xy$  states mainly hop through the  $p_z$  orbital (see Ref. 17 for more detailed discussions), and  $xz$  ( $yz$ ) via  $p_y$  ( $p_x$ ) orbitals. If there is a considerable interlayer hopping between the  $p$  orbitals, whether direct (11 family) or assisted (122 family), the ellipticity becomes  $k_z$  dependent. For instance, in  $FeSe$  there is noticeable overlap between the Se  $p_z$  orbitals, so that they form a dispersive band with the maximum at  $k_z = 0$  and the minimum at  $k_z = \pi/c$ .

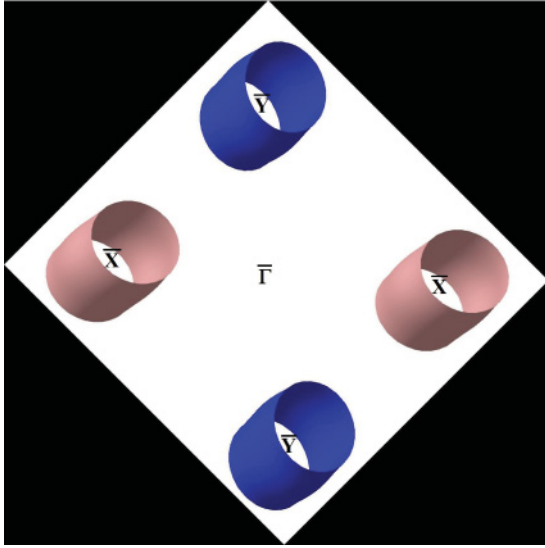


FIG. 1. (Color online) A cartoon showing a generic 3D Fermi surface for an  $\text{AFe}_2\text{Se}_2$  material in the unfolded (1 Fe/cell) Brillouin zone. Different colors show the signs of the order parameter in a nodeless  $d$ -wave state, allowed in the unfolded zone. The  $\Gamma$  point is in the center (no Fermi surface pockets around  $\Gamma$ ), and the electron pockets are around the  $\bar{X}, \bar{Y}$  points.

Obviously, hybridization is stronger when the  $p_z$  states are higher, therefore the Fermi surface ellipticity is completely suppressed in the  $k_z = 0$  plane, while rather strong in the  $k_z = \pi/c$  plane, which leads to formation of the characteristic “bellies” in the Fermi surface of FeSe. On the other hand,  $p_{x,y}$  orbitals in FeSe do not overlap in the neighboring layers, so the  $xz$  and  $yz$  bands have very little  $k_z$  dispersion, and thus the inner barrels of the electronic pockets in this compound are practically two-dimensional (2D).

In 122, the interlayer hopping proceeds mainly via the Ba (K) sites, and thus the  $k_z$  dispersion is comparable (but opposite in sign!) for the  $xy$  and  $xz/yz$  bands. As a result, when going from the  $k_z = 0$  plane to the  $k_z = \pi/c$  plane the longer axis of the Fermi pocket shrinks, and the shorter expands, so that the ellipticity actually changes sign.

Importantly, the symmetry operation that folds down the single-Fe BZ when the unit cell is doubled according to the As (Se) site symmetry is different in the 11 and 1111 structures, compared to the 122 structure. In the former case, the operation in question is the translation by  $(\bar{\pi}, \bar{\pi}, 0)$ , without any shift in the  $k_z$  direction; in the latter case, that by  $(\bar{\pi}, \bar{\pi}, \bar{\pi})$ . Thus the folded Fermi surface in 11 and in 1111 has full fourfold symmetry, while that in the 122 has such symmetry only for one particular  $k_z$ , namely,  $k_z = \pi/2c$ . Furthermore, in the 122 structure the folded bands are not degenerate along the MX line (now the labels are without the bars, that is, corresponding to the folded BZ, see Fig. 2), as they were in 11/1111. Finally, there is a considerable (at least on the scale of the superconducting gap) hybridization when the folded bands cross (except for  $k_z = 0$ ).

Now we are ready to analyze possible superconducting symmetries in the actual  $\text{AFe}_2\text{Se}_2$  materials. We do not adhere strictly to the calculated band structure and the Fermi surfaces but, rather, consider several possibilities allowed by symmetry.

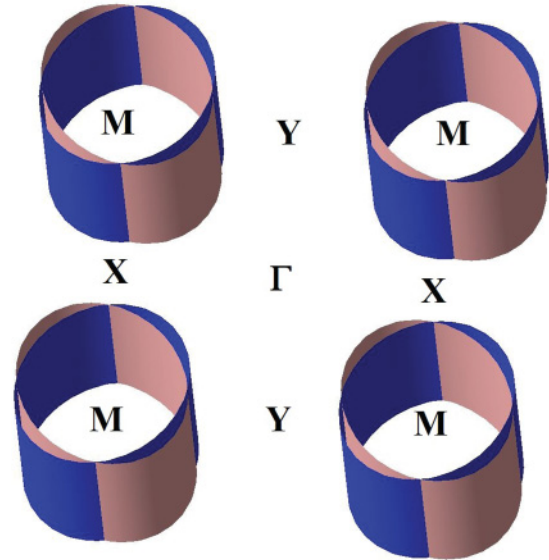


FIG. 2. (Color online) A cartoon showing a folded 3D Fermi surface for an  $\text{AFe}_2\text{Se}_2$  material, assuming a finite ellipticity, but 0  $k_z$  dispersion. Different colors show the signs of the order parameter in a  $d$ -wave state. Wherever the two colors meet, turning on hybridization due to the Se potential creates nodes in the order parameter.

Let us start first from a  $d$ -wave state in the unfolded BZ, as derived in Refs. 9, 10, and 12. In Fig. 1 we show by the two colors the signs of the order parameter. Obviously in the *unfolded* BZ such a state has no nodes.

Let us now assume that the  $k_z$  dispersion is negligible, while the ellipticity remains finite. After folding, but before turning on the hybridization, we have the picture shown in Fig. 2. The border between the red and the blue regions now becomes a nodal line.<sup>18</sup> In this case, we have four such lines for each pair of electron pockets. One can think of an effective “thickness” of the nodal lines, meaning the distance in the momentum space over which the sign of the order parameter changes. This is defined by the ratio of the hybridization gap at the point where the bands cross and their typical energy separation. Analysis of the first principle calculations for both As- and Se-based 122 compounds indicates that this ratio is varying between 0 (unless spin-orbit interaction is taken into account) and a number of the order of 1. Thus, the effect of the nodal lines on thermodynamical properties  $\text{K}_x\text{Fe}_y\text{Se}_2$  is comparable to that in one-band  $d$ -wave superconductors such as cuprates and therefore should be detectable.

Let us now gradually turn on the  $k_z$  dispersion. Nothing changes for  $k_z = \pi/2c$ , that is, there are four equidistant nodes in this plane, which we can label 1, 2, 3 and 4. As we move toward  $k_z = 0$ , nodes 1 and 3 get closer to each other, and so do nodes 2 and 4. As we move toward  $k_z = \pi/c$ , the other pairs get closer: nodes 1 and 2 and nodes 3 and 4. Thus, instead of four vertical node lines, we get four wiggly lines, otherwise similar in properties to the pure 2D case in Fig. 3. Averaged over all  $k_z$ , they still have the fourfold symmetry and the observable properties should be very similar to those in the 2D case. A notable exception is ARPES. That technique should detect gap nodes along the (0,1) and (1,0) directions when probing  $k_z = \pi/2c$ , which should gradually

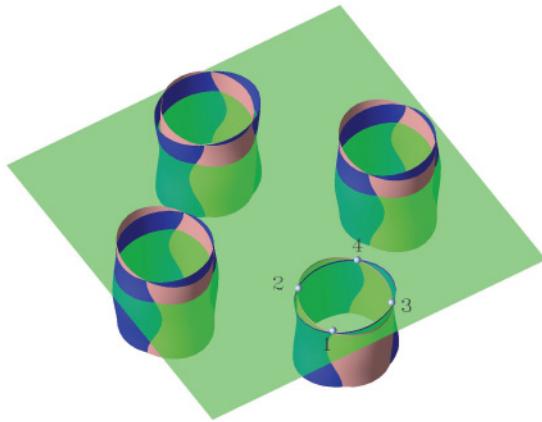


FIG. 3. (Color online) Same as Fig. 2, but assuming a moderated  $k_z$  dispersion. The plane at  $k_z = \pi/2c$  is shown, and one of the Fermi surfaces is clipped above this plane and below the  $k_z = 0$  plane, to show how the nodal points move away from their high-symmetry positions.

shift away from these directions when the probed momentum is different.

This is actually the case in density functional calculations for the stoichiometric compounds in the reported crystal structure; the intersection lines of the two Fermi surfaces folded on top of each other never close, and a  $d$ -wave superconductivity in this system must retain all four vertical node lines. Suppose, however, that these calculations underestimate the  $k_z$  dispersion (this is somewhat unlikely, as band structure calculations tend to produce overly diffuse orbitals and too much hopping, but let us assume for the sake of generality that this is possible). In that case, at some finite value of  $\tilde{k}_z$  such that  $0 < \tilde{k}_z < \pi/2c$ , nodes 1 and 2 will merge and annihilate, and so will nodes 3 and 4, while at  $k_z = \pi - \tilde{k}_z$  the other two pairs will annihilate. As a result, we will have a horizontal wiggly node line; the less wiggly, the stronger is the 3D dispersion (Fig. 4). Importantly, a full node line remains present in any band structure, whatever assumption one makes about the 3D dispersion and ellipticity. Thus, the fact that fully developed node lines are inconsistent with numerous reported

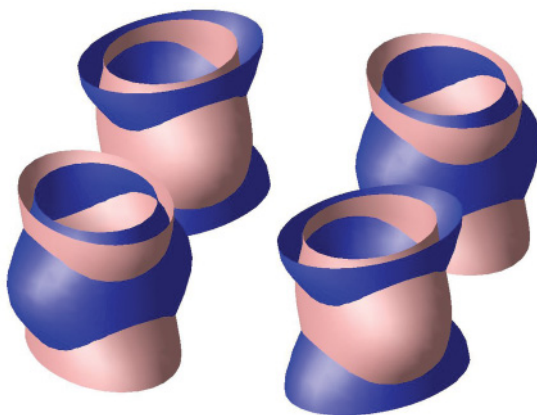


FIG. 4. (Color online) Same as Fig. 3, but assuming a very strong  $k_z$  dispersion.

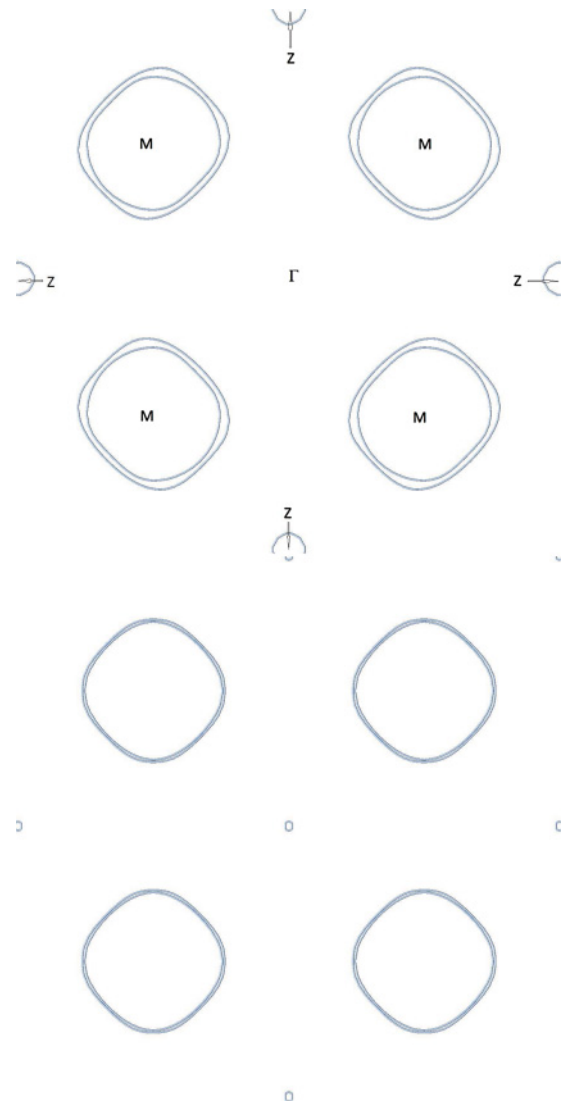


FIG. 5. (Color online) Cuts of the Fermi surfaces calculated for  $K_{0.8}Fe_2Se_2$  using the LAPW band structure in the virtual crystal approximation, and the experimental lattice parameter and atomic positions. (a)  $k_z = 0$ . (b)  $k_z = \pi/2c$  (halfway between  $\Gamma$  and  $Z$ ).

experiments cast strong doubt at  $d$ -wave pairing as a viable possibility.

An interesting alternative presents itself if we look closely at the calculated ab-initio Fermi surfaces of  $KFe_2Se_2$ . One feature that distinguishes them from those in As-based materials is their very small ellipticity and, compared to the As-based 122 family, very little  $k_z$  dispersion.<sup>19</sup> Looking at the constant- $k_z$  cuts (Fig. 5) of the Fermi surface, we observe that we are in a regime where the separation of the two Fermi surfaces is comparable to, or smaller than, the hybridization. In this case, a reasonable approximation would be to neglect both ellipticity and  $k_z$  dispersion, and analyze the possible superconducting symmetry in this model. First, in this approximation the resulting Fermi surfaces are two concentric cylinders that touch at  $k_z = 0$  but are split otherwise. The wave functions on these cylinders are, respectively, the odd and the even combinations of the original and the downfolded bands.

Thus, if the pairing interaction in the unfolded BZ exists only in the interband (interpocket) channel, as is implicitly or explicitly assumed in most current theories, it becomes identically 0 after downfolding and hybridization. In fact, in this limit, when hybridization is strong everywhere in the BZ, the spin susceptibility and the pairing interaction must be computed from scratch using the 2-Fe unit cell (and the folded BZ).

Importantly, one can easily imagine an interaction that would lead to a *nodeless* state in such a system. Indeed, if the interaction is stronger between the bonding and the antibonding band than between different points in the same band, the resulting interaction will again be a sign-changing *s* wave, with all inner barrels having one sign of the order parameter and the other the opposite sign. (A very similar state was unsuccessfully proposed for bilayer cuprates 15 years ago.<sup>20</sup>)

Note that such state cannot be distinguished from the *d*-wave state proposed in Refs. 9 and 10 by means of inelastic neutron scattering<sup>9</sup>, since it should have the same resonance below  $T_c$ , only with a twice smaller relative intensity.

Naively, one may think that one can construct a *d*-wave state where the signs of the order parameter will be swapped as one goes around from one M point in the BZ to another. Yet this is not allowed by symmetry, for  $(2\pi/a, 0, 2\pi/c)$  and  $(0, 2\pi/b, 2\pi/c)$  (2 Fe/cell notations) are reciprocal lattice vectors, so translating by any of these vectors must retain both the amplitude and the phase of the superconducting order parameter. Incidentally, this symmetry requirement is not always appreciated, and there have been “*d*-wave” suggestions (e.g., Ref. 11) that violate it.

Let us now discuss possible magnetic interactions in this system. Both from the fermiology point of view and from experiment,<sup>14</sup> it is clear that familiar spin fluctuations with the wave vector  $(\pi/a, \pi/b, q_z)$  are absent in this system. As discussed above, model calculations based on an unfolded band structure are much less well justified than in the old pnictides, at least if one believes the band structure calculations. In principle, one can controllably calculate the spin response using the full density functional theory, (DFT)<sup>21</sup> however, there are no codes widely available that implement such a capability.

On the other hand, one can gain some insight regarding the DFT spin response at  $q = 0$ , in particular, on the relative strength of the fluctuations in the ferromagnetic (FM) and in the antiferromagnetic (AFM; checkerboard) channels, in a different way. To this end, let us write the full spin susceptibility in the local density functional theory:<sup>22</sup>

$$\chi^{\text{FM}} = \frac{\chi_0^{\text{FM}}}{1 - I\chi_0^{\text{FM}}}, \quad \chi^{\text{AFM}} = \frac{\chi_0^{\text{AFM}}}{1 - I\chi_0^{\text{AFM}}}, \quad (1)$$

where  $I = 2\delta^2 E_{xc}/\delta M_{\text{Fe}}^2$  is the iron Stoner factor, which we, as the first approximation, consider independent of the magnetic pattern. Note that spin-unrestricted calculations for all magnetic patterns, FM, checkerboard, or the stripe phase, similarly to ferropnictides, converge to large magnetic moment solutions not helpful in analyzing the linear response of the nonmagnetic phase (Table I).

TABLE I. Calculated energies (the nonmagnetic state is taken as 0) for various stable and metastable magnetic states of  $\text{KFe}_2\text{Se}_2$ . Here AFM-cb refers to the antiferromagnetic checkerboard order, and stripe to the collinear order found in pnictides. FM, ferromagnetic.

	FM		AFM-cb		Stripe	
	LDA	GGA	LDA	GGA	LDA	GGA
$M_{\text{Fe}} (\mu_B)$	2.8	2.9	1.8	2.1	2.2	2.4
$\Delta E$ (meV/Fe)	+13	-140	-111	-192	-169	-290

To circumvent this problem, we use a modification of the standard LAPW package WIEN2k, which allows for a phenomenological account of itinerant spin fluctuations by tuning the Hund’s rule coupling.<sup>24</sup> It appears that the unaltered local density approximation [LDA; and even the generalized gradient approximation (GGA)] functional solution in the nonmagnetic phase is stable against weak FM perturbations (Fig. 6), even though it is unstable against the formation of a large magnetic moment.<sup>23</sup> It requires scaling  $I$  up by 40% to make it unstable, thus  $\chi_0^{\text{FM}} \approx 1/(1.4I) = 0.7/I$ . At the same time, scaling  $I$  down by  $\alpha \approx 0.7$ , we make the checkerboard pattern also marginally stable, thus  $\chi_0^{\text{AFM}} \approx 1/(0.7I) \approx 2\chi_0^{\text{FM}}$ . Thus, the fermiology favors the checkerboard AFM fluctuations about twice more than the FM ones.

This is, in some sense, encouraging. If both FM and AFM fluctuations are present, they can actually provide coupling between the bonding and the antibonding sheets of the folded Fermi surface, even if the hybridization is very strong (if only AFM fluctuations are present, this coupling vanishes in the limit of strong hybridization). It may or may not be stronger than the intraband coupling. Only full calculations of susceptibility in the two Fe unit cell will give us the answer. Yet we can firmly conclude that the only state compatible with two experimental observations, (1) that the superconducting gap does not have nodes and (2) that superconductivity emerges in the immediate proximity of an ordered magnetic phase, is again an  $s_{\pm}$  state, but this time with the order parameter

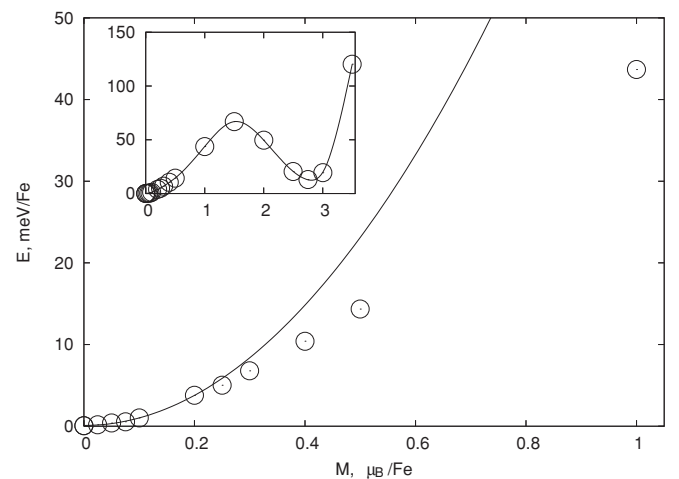


FIG. 6. Fixed spin moment calculations for the uniform (ferromagnetic) susceptibility in  $\text{KFe}_2\text{Se}_2$ . The line is the first (quadratic) term in the total energy expansion, as explained in the text. Inset: The same for large moments; here the line is a guide for the eye.

changing sign between the bonding and the antibonding state. It is also worth noting that if a 3D electron pocket is present at  $\Gamma$ , as calculations and several ARPES experiments suggest, in the proposed  $d$ -wave symmetry<sup>9-11</sup> it would be cut by four nodal lines which would also have been seen in the experiment. The concentric  $s_{\pm}$  state discussed above does not require any nodes on this pocket.

Finally, a word of caution is appropriate. While it is useful, and, arguably, imperative, at this point in time, to establish the symmetry restrictions on possible order parameter in overdoped compounds such as  $\text{AFe}_2\text{Se}_2$ , the experimental situation is by no means clear. The compositions reported range from  $\sim 0.3$  hole/Fe doped ( $\text{K}_{0.65}\text{Fe}_{1.41}\text{Se}_2$ ),<sup>25</sup> compared to the stoichiometric  $\text{AFe}_2\text{Se}_2$ , to  $\sim 0.4$  electron/Fe ( $\text{Tl}_{0.63}\text{K}_{0.37}\text{Fe}_{1.78}\text{Se}_2$ ).<sup>8</sup> A consensus seems to be emerging among experimentalists probing the bulk properties, most notably, by neutron scattering, that actual crystals occur only in a charge balance state,  $\text{K}_{2x}\text{Fe}_{2-x}\text{Se}_2$ , which is isoelectronic with  $\text{FeSe}$  and, thus, would support the now standard  $s_{\pm}$  pairing. However, this charge balance state is inconsistent with the ARPES data, on which this paper is based. Moreover, it has by now been established that in some samples the Fe vacancies order in a particular fashion,<sup>26</sup> which leads to a completely different, strongly magnetic electronic structure of a band insulator.<sup>27</sup> Experimentally the vacancy-ordered state is indeed strongly magnetic;<sup>26,28,29</sup> early claims of the coexistence of a magnetism of  $3.3 \mu_B$  per Fe with superconductivity,<sup>26,28,29</sup> something that is nearly impossible to reconcile with any theory of superconductivity, have been disputed by others,<sup>30</sup> who claim that superconductivity develops only in *disordered*

and *nonmagnetic* samples, while ordered magnetic samples are not superconducting.

Yet another caveat should be kept in mind. If the hybridization due to Se atoms is stronger than the ellipticity, as the LDA predicts, the phase space for the nodal quasiparticles in the  $d$ -wave scenario is comparable to or larger than that in a one-band  $d$ -wave superconductor. If, however, the hybridization is much smaller than the ellipticity (although so far there are no experimental or theoretical indications that this may be the case), the phase space for quasiparticles may be strongly reduced and they could be missed by typical spectroscopical probes.

To summarize the preceding paragraph, there is a deep contradiction between the ARPES band structure and that emerging from other measurements. Similarly, it has not yet been established whether superconductivity develops in a disordered structure, hopefully reasonably well described by LDA calculation in the virtual crystal approximation, or it coexists with a strongly magnetic vacancy-ordered state. While this is being sorted out, we have concentrated on the Fermi surfaces measured by ARPES and analyzed what pairing states are allowed by symmetry in this case.

#### ACKNOWLEDGMENTS

I acknowledge discussions with Andrey Chubukov, Sigfried Graser, Peter Hirschfeld, and Douglas Scalapino. I am particularly thankful to Ole Andersen and Lilia Boeri for helping me figure out the factors that control the ellipticity and the  $k_z$  dispersion in the 122 structure.

\*mazin@dave.nrl.navy.mil

<sup>1</sup>J. Guo, S. F. Jin, G. Wang, S. C. Wang, K. X. Zhu, T. T. Zhou, M. He, and X. L. Chen, *Phys. Rev. B* **82**, 180520 (2010).

<sup>2</sup>I. I. Mazin, *Physics* **4**, 26 (2011).

<sup>3</sup>L. Fang, H. Q. Luo, P. Cheng, Z. S. Wang, Y. Jia, G. Mu, B. Shen, I. I. Mazin, L. Shan, C. Ren, and H.-H. Wen, *Phys. Rev. B* **80**, 140508 (2009).

<sup>4</sup>V. Brouet, M. Marsi, B. Mansart, A. Nicolaou, A. Taleb Ibrahim, P. Le Fèvre, F. Bertran, F. Rullier-Albenque, A. Forget, and D. Colson, *Phys. Rev. B* **80**, 165115 (2009).

<sup>5</sup>I. R. Shein and A. L. Ivanovskii, e-print [arXiv:1012.5164](https://arxiv.org/abs/1012.5164); C. Cao and J. Dai, *Chin. Phys. Lett.* **28**, 057402 (2011); I. A. Nekrasov and M. V. Sadovskii, *Pisma ZhETF* **93**, 182 (2011).

<sup>6</sup>T. Qian, X.-P. Wang, W.-C. Jin, P. Zhang, P. Richard, G. Xu, X. Dai, Z. Fang, J.-G. Guo, X.-L. Chen, and H. Ding, *Phys. Rev. Lett.* **106**, 187001 (2011).

<sup>7</sup>Y. Zhang, L. X. Yang, M. Xu, Z. R. Ye, F. Chen, C. He, J. Jiang, B. P. Xie, J. J. Ying, X. F. Wang, X. H. Chen, J. P. Hu, and D. L. Feng, *Nature Materials* **10**, 273 (2011).

<sup>8</sup>X.-P. Wang, T. Qian, P. Richard, P. Zhang, J. Dong, H.-D. Wang, C.-H. Dong, M.-H. Fang, and H. Ding, *Europhys. Lett.* **93**, 57001 (2011).

<sup>9</sup>T. A. Maier, S. Graser, P. J. Hirschfeld, and D. J. Scalapino, *Phys. Rev. B* **83**, 100515(R) (2011).

<sup>10</sup>F. Wang, F. Yang, M. Gao, Z.-Y. Lu, T. Xiang, and D.-H. Lee, *Europhys. Lett.* **93**, 57003 (2011).

<sup>11</sup>T. Das and A. V. Balatsky, e-print [arXiv:1101.6056](https://arxiv.org/abs/1101.6056).

<sup>12</sup>K. Kuroki, S. Onari, R. Arita, H. Usui, Y. Tanaka, H. Kontani, and H. Aoki, *Phys. Rev. Lett.* **101**, 087004 (2008).

<sup>13</sup>B. Zeng, B. Shen, G. F. Chen, J. B. He, D. M. Wang, C. H. Li, and H.-H. Wen, *Phys. Rev. B* **83**, 144511 (2011).

<sup>14</sup>L. Ma, J. B. He, D. M. Wang, G. F. Chen, and W. Yu, *Phys. Rev. Lett.* **106**, 197001 (2011).

<sup>15</sup>R. H. Yuan, T. Dong, G. F. Chen, J. B. He, D. M. Wang, and N. L. Wang, e-print [arXiv:1102.1381](https://arxiv.org/abs/1102.1381).

<sup>16</sup>P. A. Lee and X.-G. Wen, *Phys. Rev. B* **78**, 144517 (2008).

<sup>17</sup>O. K. Andersen and L. Boeri, *Ann. Phys.* **523**, 8 (2011).

<sup>18</sup>Doubling of a unit cell and corresponding downfolding of the BZ do not necessarily lead to formation of nodes. However, it was shown by D. Parker, M. G. Vavilov, A. V. Chubukov, and I. I. Mazin [*Phys. Rev. B* **80**, 100508 (2009)] that if the symmetry lowering occurs in the charge channel (charge density wave), hybridization of bands with the opposite signs of the order parameter leads to gap nodes, while if it occurs in the spin channel, the nodes are avoided. Symmetry lowering due to Se ions occurs in the charge channel and thus nodal lines are necessarily formed.

<sup>19</sup>This is true for my own calculations, which were performed in the experimental crystal structure using the standard WIEN2k band structure package, as well as for other reported calculations,<sup>5</sup> although pseudopotential calculations reported in Ref. 9 have a somewhat stronger  $k_z$  dispersion.

<sup>20</sup>A. I. Liechtenstein, I. I. Mazin, and O. K. Andersen, *Phys. Rev. Lett.* **74**, 2303 (1995).

- <sup>21</sup>S. Y. Savrasov, *Phys. Rev. Lett.* **81**, 2570 (1998).
- <sup>22</sup>There are a number of simplifications in this expression, for instance, we have neglected the so-called local field effects and possible  $\mathbf{q}$  dependence of the Stoner factor  $J$ , but these simplifications are not principal for our qualitative estimate.
- <sup>23</sup>Incidentally, the same is true for the “stripe” phase, the pattern that is the ground state in our calculations and is observed experimentally in pnictides. While the large-moment solution is very stable, the nonmagnetic state is stable against small perturbations of this symmetry, not only in the LDA but also in the GGA.
- <sup>24</sup>This is implemented by the following recipe: first, at each iteration, the standard LDA or GGA potential for the spin-up and spin-down channel is calculated; then it is rescaled according to the formula  $v_{\uparrow}(\mathbf{r}) = [v_{\uparrow}(\mathbf{r}) + v_{\downarrow}(\mathbf{r})]/2 + \alpha[v_{\uparrow}(\mathbf{r}) - v_{\downarrow}(\mathbf{r})]/2 = v_{\uparrow}(\mathbf{r})(1 + \alpha)/2 + v_{\downarrow}(\mathbf{r})(1 - \alpha)/2$ ,  $v_{\downarrow}(\mathbf{r}) = v_{\uparrow}(\mathbf{r})(1 - \alpha)/2 + v_{\downarrow}(\mathbf{r})(1 + \alpha)/2$ , where  $0 \leq \alpha \leq 1$ .
- <sup>25</sup>D. A. Torchetti, M. Fu, D. C. Christensen, K. J. Nelson, T. Imai, H. C. Lei, and C. Petrovic, *Phys. Rev. B* **83**, 104508 (2011).
- <sup>26</sup>W. Bao, Q. Huang, G. F. Chen, M. A. Green, D. M. Wang, J. B. He, X. Q. Wang, and Y. Qiu, e-print [arXiv:1102.0830](https://arxiv.org/abs/1102.0830); V. Yu. Pomjakushin, E. V. Pomjakushina, A. Krzton-Maziopa, K. Conder, and Z. Shermadini, *J. Phys. Condens. Matter* **23**, 156003 (2011); F. Ye, S. Chi, Wei Bao, X. F. Wang, J. J. Ying, X. H. Chen, H. D. Wang, C. H. Dong, and Minghu Fang, e-print [arXiv:1102.2882](https://arxiv.org/abs/1102.2882).
- <sup>27</sup>X.-W. Yan, M. Gao, Z.-Y. Lu, and T. Xiang, *Phys. Rev. B* **83**, 233205 (2011).
- <sup>28</sup>Z. Li, X. Ma, H. Pang, and F. Li, e-print [arXiv:1103.0098](https://arxiv.org/abs/1103.0098); D. H. Ryan, W. N. Rowan-Weetaluktuk, J. M. Cadogan, R. Hu, W. E. Straszheim, S. L. Bud’ko, and P. C. Canfield, e-print [arXiv:1103.0059](https://arxiv.org/abs/1103.0059).
- <sup>29</sup>Z. Shermadini, A. Krzton-Maziopa, M. Bendele, R. Khasanov, H. Luetkens, K. Conder, E. Pomjakushina, S. Weyeneth, V. Pomjakushin, O. Bossen, and A. Amato, *Phys. Rev. Lett.* **106**, 117602 (2011).
- <sup>30</sup>F. Han, B. Shen, Z.-Y. Wang, and H.-H. Wen, e-print [arXiv:1103.1347](https://arxiv.org/abs/1103.1347).